Hindawi
Wireless Communications and Mobile Computing
Volume 2020, Article ID 8841210, 12 pages
https://doi.org/10.1155/2020/8841210

Research Article

Analysis and Optimization of Asymmetric Wireless Power Transfer in Concrete

Zijian Tian,[1] Dairong Liu,[1] Wei Chen,[1,2] Wenqing Wang,[3] Shan Pan,[1] and Ni Guo[1]

[1]*School of Mechanical Electronic & Information Engineering, China University of Mining and Technology (Beijing), Beijing 100083, China*
[2]*School of Computer Science and Technology, China University of Mining and Technology, Xuzhou, Jiangsu 221000, China*
[3]*Beijing Polytechnic College, Beijing 100042, China*

Correspondence should be addressed to Wei Chen; chenwdavior@163.com

Received 31 August 2020; Revised 2 November 2020; Accepted 25 November 2020; Published 10 December 2020

Academic Editor: Chi-Hua Chen

With the rapid development of the Internet of things (IoT) technology, the application of IoT has been expanded greatly, and the disadvantages of the traditional battery power supply have become increasingly prominent. The power supply mode limits the development of the concrete structural health monitoring network. And the application of magnetic resonance coupled wireless power transfer technology can solve the problem of power supply to sensors embedded in concrete. The corrected transmission efficiency considering the concrete conductivity is proposed which establishes the relationship between the electromagnetic field and the circuit model. And the field-circuit coupled model of asymmetric wireless power transfer system in concrete is developed. The effects of radial offset and axial dislocation on the transmission efficiency at different concrete conductivity are further analyzed. The relationship between the resonant frequency and the transmission efficiency in different concrete conductivity is analyzed, and an optimization scheme is proposed to improve the transmission efficiency. Finally, the experimental setups are established, and the theoretical analysis is verified. The conclusions cannot only break through the bottleneck of the scale of the concrete structural health monitoring network but also further releases the application potential of IoT.

1. Introduction

In recent years, Internet of things (IoT) technology has been applied in many fields of our life. With the development of application, different IoT specifications and semantic mobile computing technologies have emerged [1–3]. The stable power supply of each part is the basis for realizing the service interoperability between different platforms. Lithium batteries are widely used in the field of wearable devices and industrial IoT, and the mainstream development trend is to reduce the loss current by simulating the design technology and power system technology to extend the system operation time and standby time. But the current power solutions cannot fundamentally solve the problem of system interruption caused by battery charging and replacement. In the field of Internet of vehicles, the power system needs to adopt a combined integrated power management solution with the increasing number of onboard intelligent modules to achieve stronger system power performance. But the transmission speed of information still poses a great technical challenge to the power solution.

The concrete structural health monitoring network is capable to realize the damage identification and the safety judgment for buildings, bridges, and tunnels through kinds of sensors embedded in concrete that collects real-time data and upload the data to the information processing center. Continuous and stable operation of system can be realized by introducing contactless power transfer technology, which can avoid the corrosion of concrete to damage power supply cable of sensors. And the cost of battery replacement can also be reduced for the battery-powered sensors embedded in concrete. This technology can be extended to the whole field of the IoT which can increase the coverage of IoT and reduce the production cost of products. It can also provide a new

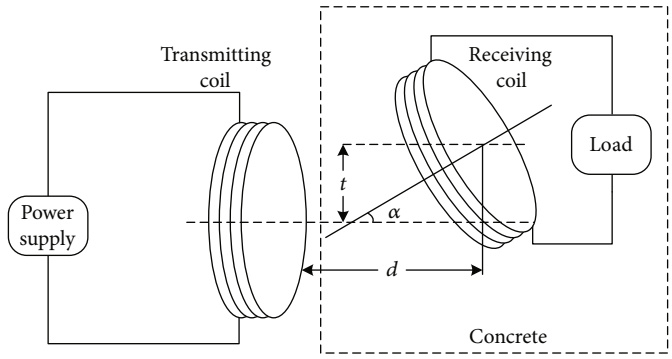

Figure 1: Asymmetric wireless power transfer system in concrete.

power solution for the IoT ecosystem. The landmark of contactless power transfer from concept to application was the proposal of magnetic resonance-coupled wireless power transfer which achieved efficient midrange power transfer [4]. Since then, scientists began to explore and research this emerging field and had considerable achievements [5–8]. The application of technology can further promote the development of the concrete structural health monitoring network.

A high-frequency rectangular patch antenna was proposed to demonstrate the feasibility of wireless power supply to sensors embedded in concrete in [9]. The problem of wireless power supply to sensors embedded in concrete was solved by the application of wireless power transfer technology in [10]. And the experimental setup was built to verify the transmission performance. Steel bars in concrete were proposed as the medium of low-frequency magnetic induction to realize long-distance wireless power transfer in [11]. The wireless power transfer system that the resonant frequency was fixed at 60 Hz was built in [12]. And the efficiency formula including copper core losses in concrete was derived, and the effect of the shape of magnet pole pieces on the transmission performance was analyzed. The effect of reinforced concrete widely used in metro construction on the transmission performance was analyzed in [13]. And the unnecessary loss including dielectric loss, the hysteresis loss, and the eddy current loss was derived through analytical formula and finite element analysis. The result showed the eddy current loss was the main reason of performance degradation. A novel multicoil resonator was designed which was capable to solve the problem of low transmission efficiency in [14]. And the interference of reinforcement array was canceled through adding the four middle coils to a certain extent. The transmission efficiency was compared between the system in dry concrete and free space in [15]. And the output power was measured in different concrete medium when the input power was constant. The models of the low power near-field system in dry and wet concrete were established in [16]. And the DC current and output power gradually increased with the drying of wet concrete. The wireless power transfer system in concrete was developed in [17]. And the concrete material mixed in a certain proportion was verified to improve the transmission performance. The effects of the height of transmitting coil, the depth of receiving coil, and the concrete humidity on the transmission performance were analyzed by the extended Debye model in [18]. The radial offset and axial dislocation between the coils are common asymmetrical conditions, which are important factors that cause the change of transmission performance. The formulas of self-inductance and mutual inductance of circular coil in near field wireless power transfer were given in [19]. And the formulas of the mutual inductance and the transmission efficiency in the case of misalignment also were derived, and the effect of radial offset and angular misalignment was studied. A mathematical model of wireless power transfer system with series-parallel compensation network was developed, which was capable to determine the circuit parameters under various misalignment conditions in [20]. And the mathematical model was used to realize the preliminary design of the system. The mutual inductance formulas in the case of radial offset, axial dislocation, and general misalignment between the coils were derived, and the relationship between the optimal transmission performance and the turns of the coils was defined in [21]. The change of transmission performance when the misalignment occurs was analyzed, and an optimization scheme was proposed to improve the transmission efficiency by changing the relative position between the coils in [22]. A novel coil structure was designed to realize stable transmission performance with the varying of angular misalignment in [23, 24]. A multivariable dynamic tuning method was proposed in [25]. And the maximum output power point was tracked through monitoring the size and phase of the inductance current.

In Section II, the eddy current equivalent resistance and corrected mutual inductance voltage is presented, and the corrected transmission efficiency formula is analyzed. In Section III, the asymmetric wireless power transfer in different concrete conductivity is analyzed, and an optimization scheme to improve the transmission efficiency is proposed. In Section IV, the experimental setups are established, and the theoretical analysis is verified. In Section V, the results are listed. In Section VI, the paper is summarized and the limitations are elaborated.

2. Theoretical Analysis

The schematic diagram of asymmetric wireless power system in concrete is shown in Figure 1. Here, t is the radial offset

distance, and α is the dislocation angle. And the receiving coil is sealed in concrete. The concrete medium has different conductivity due to the different humidity environment and manufacturing process. The conductivity of concrete medium is generally 0.4-5 S/m. There is sinusoidal alternating current in the transmitting loop and the receiving loop.

The sinusoidal alternating electromagnetic field generated by the sinusoidal alternation current is periodic field with the variation of time. And the complex Maxwell equations can omit the process of solving the time, reduce the complexity of solution, and realize the transformation from the time domain to frequency domain.

The complex Maxwell equations are as follows:

$$\begin{cases} \nabla \times H = \sigma E + j\omega\varepsilon E \\ \nabla \times E = -j\omega\mu H \\ \nabla \cdot \mu H = 0 \\ \nabla \cdot \varepsilon E = \rho, \end{cases} \tag{1}$$

where E is the electric field strength, H is the magnetic field strength, σ is the conductivity, μ is the permeability, and ε is the dielectric constant of the medium. According to (1) and (2), the constraint equation of electric field can be derived as follows:

$$\nabla \times (\nabla \times E) = \nabla(\nabla \cdot E) - \nabla^2 E, \tag{2}$$

$$\begin{cases} \nabla^2 E + \dfrac{1}{\sigma + j\omega\varepsilon} \nabla(\nabla \cdot \sigma E) = j\omega\mu(2\sigma + j\omega\varepsilon)E \\ \nabla \cdot E + \dfrac{1}{\sigma + j\omega\varepsilon} \nabla \cdot \sigma E = 0. \end{cases} \tag{3}$$

The electromagnetic field model of the coil is built in the cylindrical coordinate system, and the coordinates of any point in the field are (ρ, φ, z). The radius of the coil is r, and the effective value of the sinusoidal alternating current is I. The distance from the xOy plane is d, and the axial of the coil coincides with z-axis. The field is divided into two parts by the plane of the coil for ensuring that no external source in the solution area. And the boundary value problem of electric field is analyzed. Since the electric field is the eddy electric field parallel to the plane of the coil, the boundary value problem of electric field can be simplified as the boundary value problem of circumferential component of electric field.

According to (3), the constraint equation of electric field is simplified as follows:

$$\nabla^2 E_\phi - \frac{j\omega\mu(\sigma + j\omega\varepsilon) + 1}{\rho^2} E_\phi = 0. \tag{4}$$

Boundary conditions for the plane of the coil are expressed as follows:

$$\begin{aligned} E_{2\phi} - E_{1\phi} &= 0, \\ \frac{\partial E_{2\phi}}{\partial z} - \frac{\partial E_{1\phi}}{\partial z} &= j\omega\mu I \delta(\rho - r). \end{aligned} \tag{5}$$

Boundary condition for the infinite far place is expressed as follows:

$$\lim_{x \to \infty} eE_\phi = c_\phi, \tag{6}$$

where e is the distance from the coordinate origin to the point (ρ, φ, z) and c is the bounded constant vector independent of the coordinate system. By solving the ordinary differential equation, the electric field strength E is obtained from the above boundary conditions as follows:

$$E = -\frac{j\omega\mu r I}{2} \int_0^\infty \frac{\lambda J_1(\lambda r) J_1(\lambda \rho)}{\sqrt{\lambda^2 + j\omega\mu(\sigma + j\omega\varepsilon)}} e^{(z-d)\sqrt{\lambda^2 + j\omega\mu(\sigma + j\omega\varepsilon)}} d\lambda e_\varphi. \tag{7}$$

And the eddy current loss generated by the eddy electric field is as follows:

$$P_{Loss} = \int_v \sigma E^2 dv, \tag{8}$$

Where v is the solution area of eddy current loss between the coils.

According to (7) and (8), the eddy current loss is directly proportional to the square of the effective value of current. Therefore, the eddy current equivalent resistance is defined as the eddy current loss divided by the square of the effective value of current as follows:

$$R_{\text{Loss}} = \frac{P_{\text{Loss}}}{I^2}, \tag{9}$$

where R_{Loss} is a function of conductivity. The relationship between the electromagnetic field and the circuit model is established by the eddy current equivalent resistance which can simplify the analysis parameters and process. And it is easier to analyze the effect of concrete conductivity on the transmission efficiency.

The asymmetric coil model is shown in Figure 2. The radial offset and axial dislocation affect the mutual inductance between the coils and further reduce the transmission efficiency. In [22], the mutual inductance formula for radial offset and axial dislocation was derived as follows:

$$M = \frac{\mu_0 n_1 n_2}{4\pi} \int_0^{2\pi} \int_0^{2\pi} \frac{r_1 r_2 (\sin\theta \sin\varphi \cos\alpha + \cos\theta \cos\varphi) d\theta d\varphi}{R_{QN}}, \tag{10}$$

where the cylindrical coordinate system is adopted and the coordinates of the center of the receiving coil are $(0, t, d$

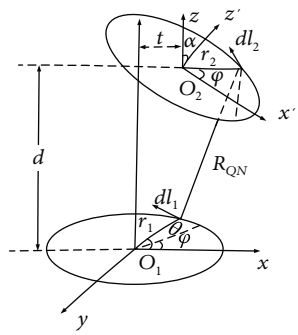

Figure 2: Asymmetric coil model.

). The mutual inductance voltage phase is 90° behind the excitation current phase in the air, but the mutual inductance voltage phase is no longer 90° behind the excitation current phase in concrete, and the effective value also has changes. The mutual inductance voltage formula in concrete is corrected, and the formula is as follows:

$$U^{12}_{\text{concrete}} = -f(\sigma)j\omega M I_{\text{concrete}} e^{-j\beta}, \tag{11}$$

where $f(\sigma)$ is a function of conductivity which is defined as the correction coefficient of the effective value and β is the difference of electric field strength phase between air and concrete. There are two differences between the circuit model and the corrected model: the eddy current equivalent resistance and corrected mutual inductance voltage as shown in Figure 3. U_S is the high-frequency voltage source. R_1 and R_2 are the equivalent resistance of the transmitting loop and the receiving loop. L_1 and L_2 are the self-inductance of the transmitting coil and the receiving coil. C_1 and C_2 are the equivalent compensation capacitance. R_{Loss1} and R_{Loss2} are the eddy current equivalent resistance. M is the mutual inductance between the coils. R_L is the equivalent load resistance.

According to Kirchhoff's law, the voltage equations can be expressed as follows:

$$\begin{aligned} U_1 &= I_1 R_1 + I_1 R_{\text{Loss1}} + j\omega L_1 I_1 + \frac{1}{j\omega C_1} I_1 - f(\sigma)j\omega M I_2 e^{-j\beta}, \\ -f(\sigma)j\omega M I_1 e^{-j\beta} &= j\omega L_2 I_2 + I_2 R_{\text{Loss2}} + I_2 R_2 + I_2 R_L + \frac{1}{j\omega C_2} I_2. \end{aligned} \tag{12}$$

In order to facilitate the calculation, assuming $R_1 = R_2 = R$, $C_1 = C_2 = C$, and $L_1 = L_2 = L$. And the current of the transmitting loop and the receiving loop is as follows:

$$\begin{aligned} I_1 &= \frac{(j\omega L + R + R_{\text{Loss2}} + R_L + (1/j\omega C))U_1}{(j\omega L + R + R_{\text{Loss2}} + R_L + (1/j\omega C))(j\omega L + R + R_{\text{Loss1}} + (1/j\omega C)) + f(\sigma)^2\omega^2 M^2 e^{-j2\beta}}, \\ I_2 &= \frac{f(\sigma)j\omega M e^{-j\beta} U_1}{(j\omega L + R + R_{\text{Loss2}} + R_L + (1/j\omega C))(j\omega L + R + R_{\text{Loss1}} + (1/j\omega C)) + f(\sigma)^2\omega^2 M^2 e^{-j2\beta}}. \end{aligned} \tag{13}$$

The transmission efficiency is determined as follows:

$$\eta = \frac{f(\sigma)^2\omega^2 M^2 e^{-j2\beta} R_L}{\left[(R + R_{\text{Loss1}})(R + R_L + R_{\text{Loss2}}) + f(\sigma)^2\omega^2 M^2 e^{-j2\beta}\right](R + R_L + R_{\text{Loss2}})}. \tag{14}$$

The transmission efficiency formula considering the concrete conductivity is derived which shows that the concrete conductivity is an important factor that causes the change of transmission performance. It is mainly reflected by the eddy current equivalent resistance and corrected mutual inductance voltage. Also, the radial offset and axial dislocation between the coils are common asymmetrical conditions in the specific engineering. Therefore, it is necessary to study the effect of radial offset and axial dislocation between the coils on the transmission efficiency at different concrete conductivity.

3. Establishment and Analysis of System Model

In this section, Maxwell and Simplorer are used to establish the model of asymmetric wireless power transfer system with the transmitting coil in the air and the receiving coil in the concrete. The three-dimensional system model established in Maxwell is shown in Figure 4. And the design parameters are shown in Table 1.

In order to study the effect of the conductivity of concrete medium, the dry concrete, wet concrete, and reinforced concrete is used as the transmission mediums. According to the normal standard parameters, the conductivity is set to 1 S/m, 3.8 S/m, and 4.9 S/m, respectively. The three-dimensional system model is imported into the external circuit that established in Simplorer. The stop time is 10 μs, the time step is 0.02 μs, and the circuit parameters are shown in Table 2.

The spatial distribution of magnetic flux density at different radial offset distance is shown in Figure 5. In Figure 5, the magnetic field is mainly distributed inside the coils and between the coils, indicating that the transmission of energy is achieved through the coupling of magnetic field. The magnetic flux density of the transmitting coil increases from 1.1232×10^{-4} T to 1.7974×10^{-4} T throughout the process, which shows that the energy of the transmitting coil cannot be effectively transmitted to the receiving coil with the increase of radial offset distance. In addition, the effect of concrete medium on the spatial distribution of magnetic flux

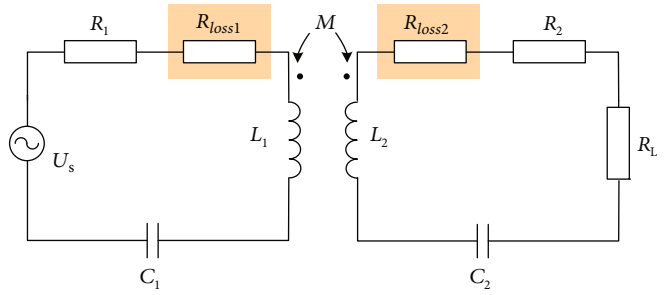

Figure 3: Corrected circuit mutual inductance model in concrete.

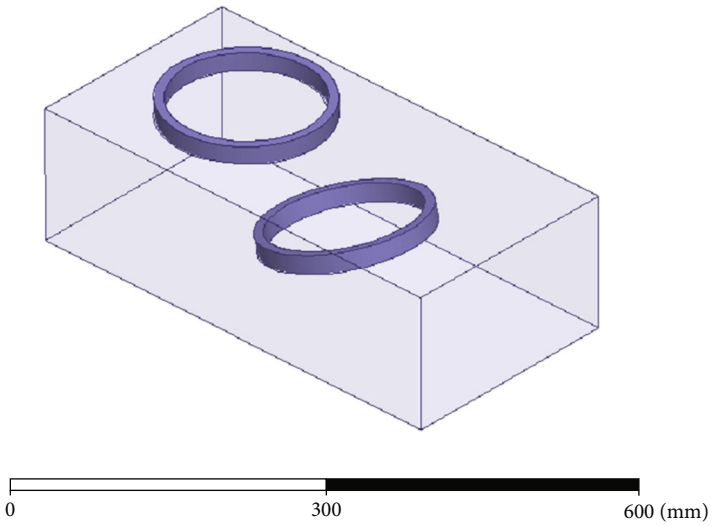

Figure 4: Three-dimensional system model.

Table 1: Design parameters.

	Value
Internal diameter	80 mm
External diameter	90 mm
Wire diameter	2 mm
Turns	5 turns
Axial distance	80 mm
Concrete size ($L \times W \times H$)	$500 \times 250 \times 150$ mm

Table 2: Circuit parameters.

	Transmitting loop	Receiving loop
Resonant frequency	6 MHz	
Resistance	0.2 Ω	
Power supply voltage	18 V	—
Load	—	50 Ω
Self-inductance	72.19 μH	70.92 μH
Matching capacitance	9.74 pF	9.92 pF

density always exists. The magnetic flux density is obviously weakened at the interface between concrete and air. And the weakening trend is more obvious with the increase of radial offset distance, which shows that the transmission of energy is hindered by concrete medium to a certain extent.

The simulation current can be obtained at different conditions through the Maxwell and Simplorer joint simulation method. The current simulation waveform when the radial offset distance $t = 0$ mm in dry concrete is shown in Figure 6.

The effect of radial offset on the transmission efficiency in different concrete medium is shown in Figure 7. The transmission efficiency remains almost constant when the radial offset is in a small scope. With the increase of radial offset distance, the transmission efficiency decreases dramatically. The effect of concrete conductivity on the transmission efficiency is also significant. The transmission efficiency has overall increase with the continuous decrease of concrete conductivity. Compared with wet and reinforced concrete, the energy can be transmitted in dry concrete at a longer radial offset distance. And the trend of transmission efficiency is identical in different concrete conductivity with the increase of radial offset distance, which confirms the relationship between the eddy current loss and conductivity in the eddy current loss formula, which further proves that the eddy current loss is an important factor that causes the change of transmission performance.

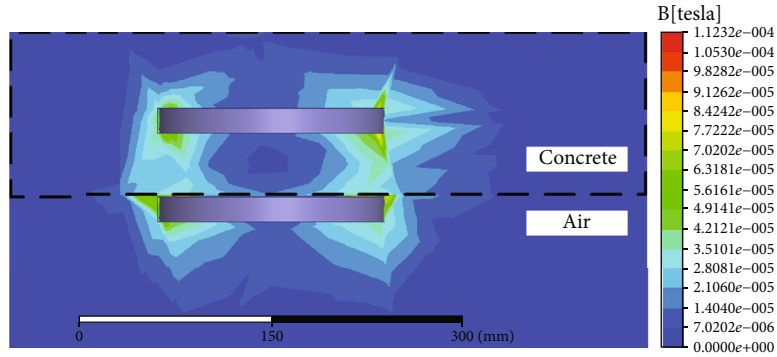

(a) $t = 0$ mm

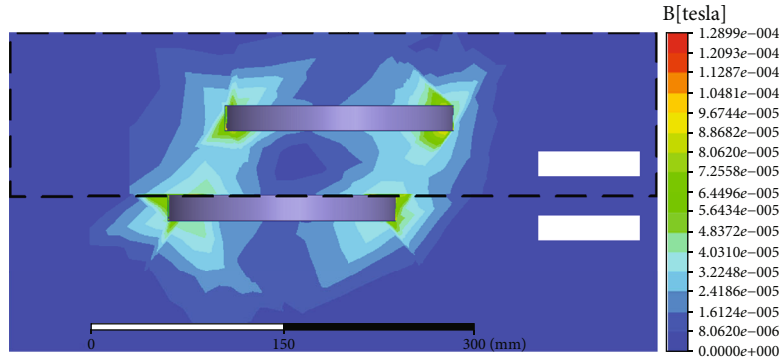

(b) $t = 45$ mm

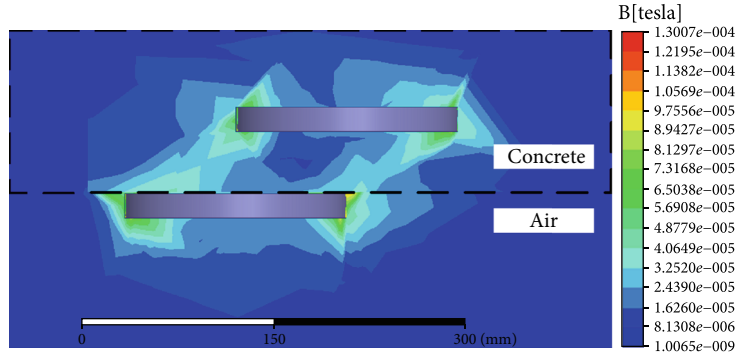

(c) $t = 90$ mm

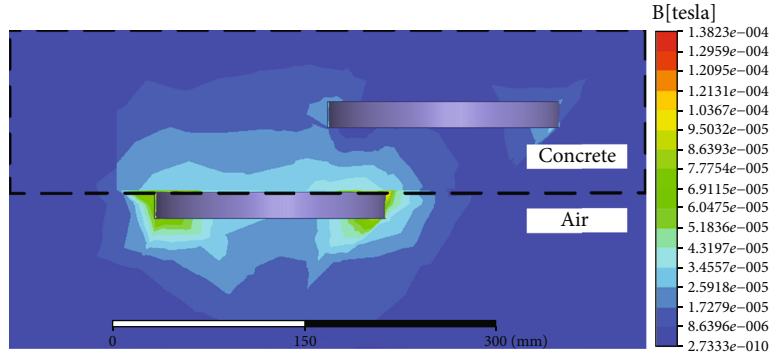

(d) $t = 135$ mm

Figure 5: Continued.

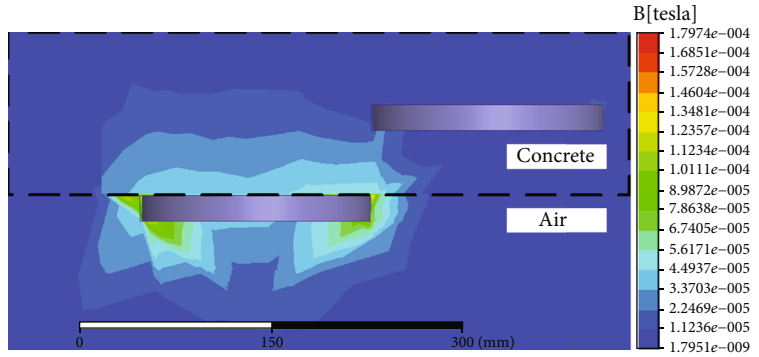

(e) $t = 180$ mm

Figure 5: The spatial distribution of magnetic flux density at different radial offset distance.

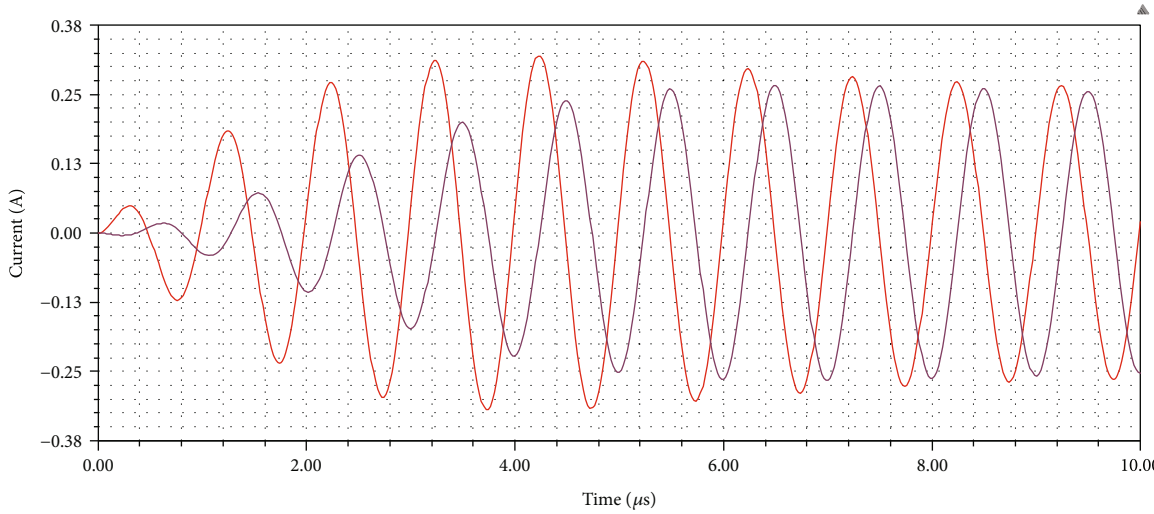

Curve Info	rms
Current (Phase_prim) Setup1 : Transient	0.1926
Current (Phase_sec) Setup1 : Transient	0.1829

Figure 6: Current simulation waveform of the two coils in dry concrete when $t = 0$ mm.

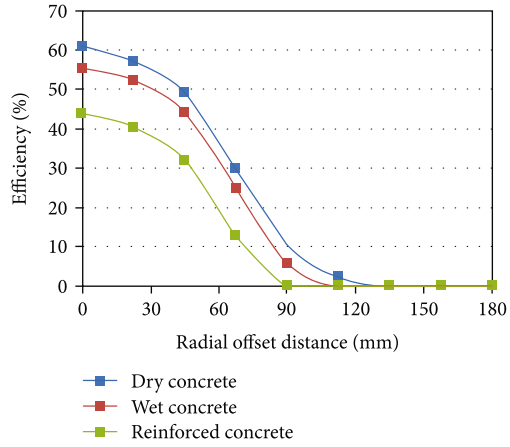

Figure 7: The effect of radial offset on the transmission efficiency in different concrete medium (dry concrete $\sigma = 1$ S/m, wet concrete $\sigma = 3.8$ S/m, and reinforced concrete $\sigma = 4.9$ S/m).

The spatial distribution of magnetic flux density at different dislocation angle is shown in Figure 8. In Figure 8, the magnetic field is mainly distributed inside the coils and between the coils, indicating that the transmission of energy is achieved through the coupling of magnetic field. The magnetic flux density of the whole system remains almost constant with the increase of dislocation angle α from 0° to 45° indicating that the transmission performance does not change much. In addition, the magnetic flux density is also weakened at the interface between concrete and air. Since the magnetic flux density remains almost constant, the weakening trend is not obvious with the increase of dislocation angle.

The effect of axial dislocation on the transmission efficiency in different concrete medium is shown in Figure 9. When the dislocation angle α varies from 0° to 45°, the transmission performance remains steady and the fluctuation of

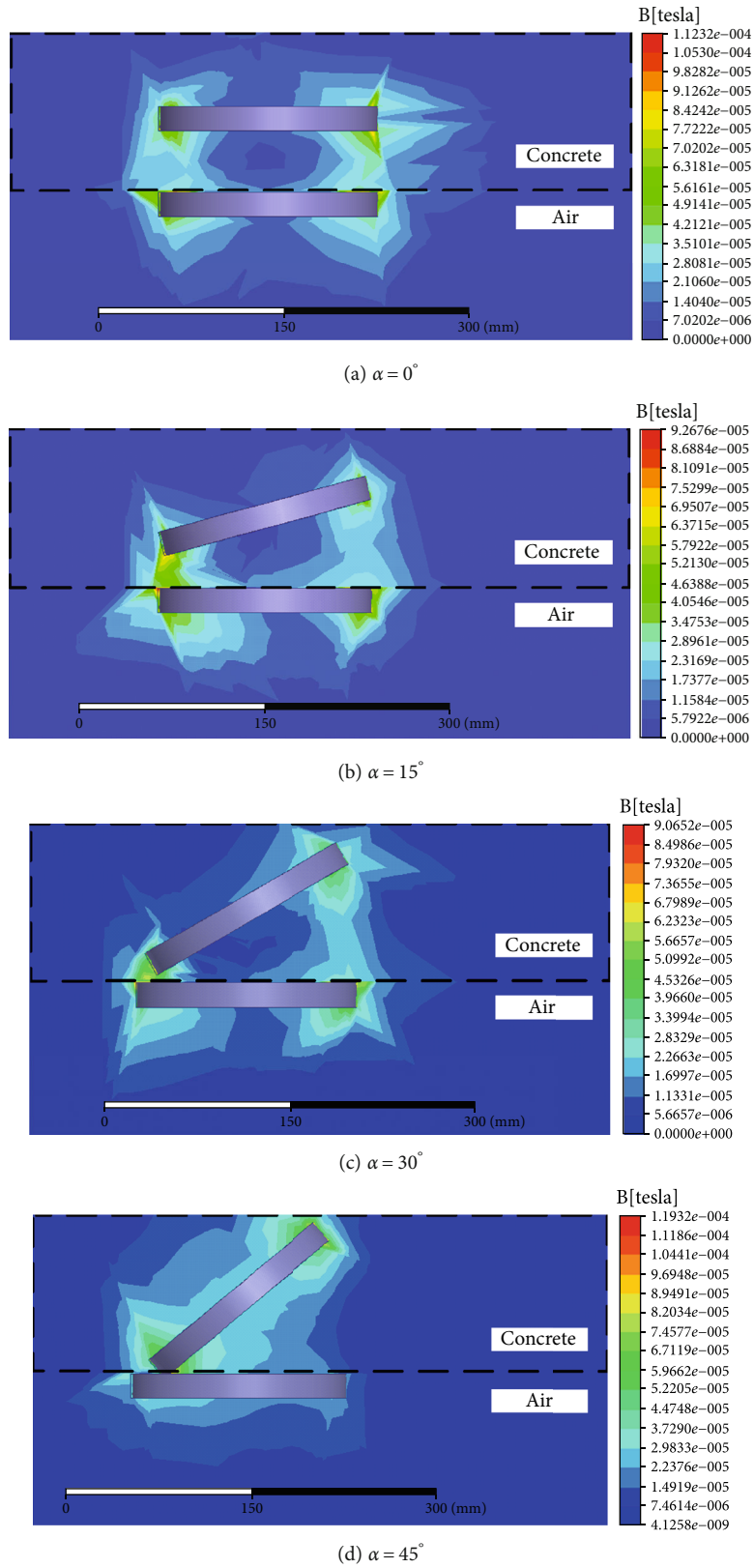

Figure 8: The spatial distribution of magnetic flux density at different dislocation angle.

the transmission efficiency is small. Figure 9 still shows that the eddy current loss is an important factor that causes the change of transmission performance.

Figure 10 shows that the effect of resonant frequency on the transmission efficiency in different concrete medium. The transmission efficiency drops sharply with the increase

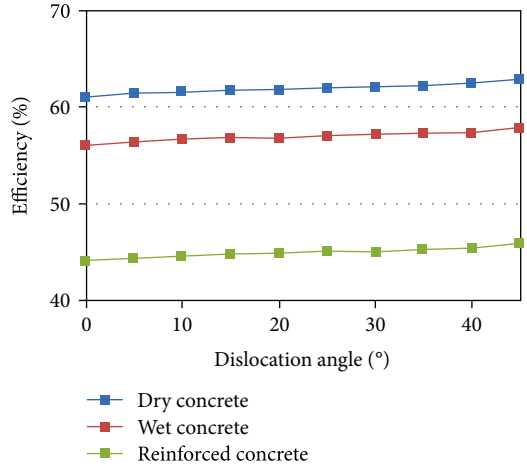

Figure 9: The effect of axial dislocation on the transmission efficiency in different concrete medium (dry concrete $\sigma = 1$ S/m, wet concrete $\sigma = 3.8$ S/m, and reinforced concrete $\sigma = 4.9$ S/m).

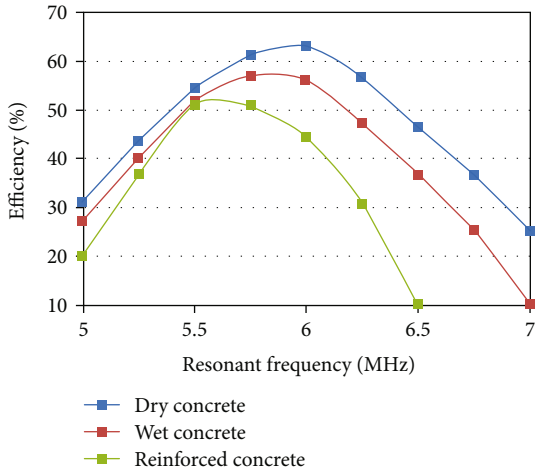

Figure 10: The effect of resonant frequency on the transmission efficiency in different concrete medium (dry concrete $\sigma = 1$ S/m, wet concrete $\sigma = 3.8$ S/m, and reinforced concrete $\sigma = 4.9$ S/m).

of conductivity at the same resonant frequency which further confirms the correctness of the conclusion analyzed from Figures 7 and 9. The optimal resonant frequency in dry concrete is approximately 5.93 MHz. The optimal resonant frequency in wet concrete is approximately 5.82 MHz. And the optimal resonant frequency in reinforced concrete is approximately 5.54 MHz. It shows that the optimal resonant frequency is gradually decreasing with the increase of conductivity. Therefore, the frequency shift is also an important factor that causes the change of transmission performance. According to the change rule of the transmission efficiency and the optimal resonant frequency in different concrete conductivity, an optimization scheme to improve the transmission efficiency is proposed. When the transmission efficiency is lower than the normal transmission standard in engineering due to the change of coil position or the difference of concrete conductivity, the transmission efficiency can be improved by properly reducing the resonant frequency to close the optimal resonant frequency. Figure 11 shows that the transmission efficiency can be improved in reinforced concrete by this optimization scheme. And compared with dry and wet concrete, the transmission efficiency has a great improvement in the reinforced concrete. Therefore, this optimization scheme is more effective for the system with high conductivity.

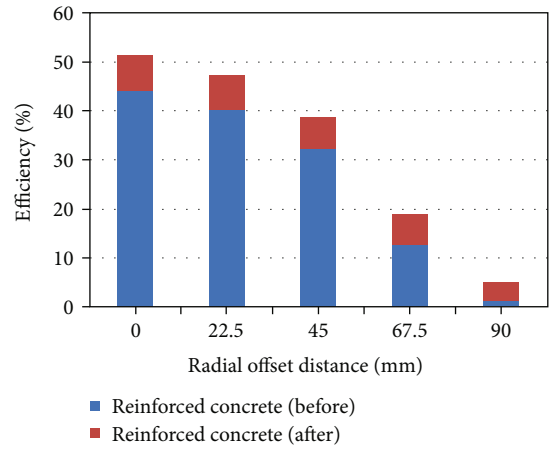

Figure 11: The effect of the optimization scheme in reinforced concrete (reinforced concrete $\sigma = 4.9$ S/m).

4. Experimental Validation

The experimental setups of wireless power transfer system are shown in Figure 12. The digital signal generator, the power amplifier, and the DC power supply constitute a high-frequency power supply which provides energy for magnetic resonance coupled wireless power transfer system. The impedance matching device ensures the optimal transmission performance before the experiments. The transmitting coil and the receiving coil are two identical coils, and the parameters of the coils are given as follows: wire diameter 2 mm, coil radius 90 mm, and 5 turns. To satisfy the experimental requirements, the receiving coil and load is sealed in the concrete. In order to study the effect of the conductivity of concrete medium, the dry concrete, wet concrete, and reinforced concrete are used as the transmission medium. The conductivity of the dry concrete, wet concrete, and reinforced concrete is measured as 1.31 S/m, 3.63 S/m, and 4.97 S/m. The load is a resistance box of the type EMC5307ALN, and the resistance value is 50 Ω.

The identical resonant frequency is a precondition for magnetic resonance coupled wireless power transfer, and the resonant frequency of the system is adjusted to 6 MHz by adding the corresponding compensation capacitance. The axial distance between the coils is always fixed at 80 mm during the experiment. Figure 13 shows that the effect of resonant frequency on the transmission efficiency in different concrete medium. The effects of the conductivity of concrete medium on the transmission efficiency from big to small are reinforced concrete, wet concrete, and dry concrete. And the optimal resonant frequency in different concrete

Figure 12: Experimental setups of wireless power transfer system in concrete.

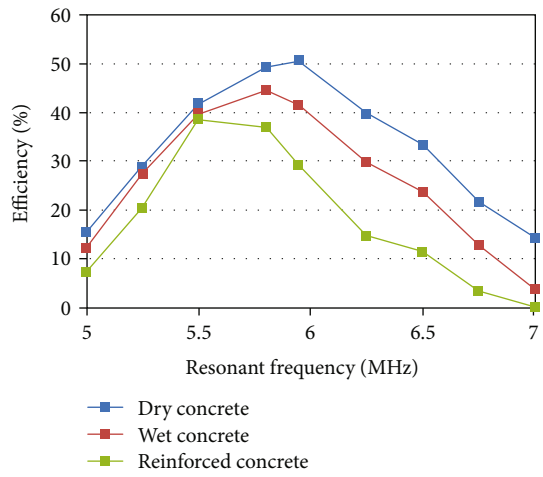

Figure 13: The effect of resonant frequency on the transmission efficiency in different concrete medium.

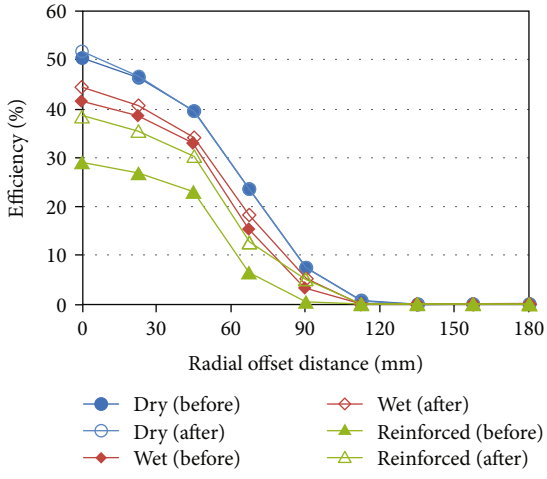

Figure 14: The effect of radial offset on the transmission efficiency in different concrete medium.

conductivity also changes. The optimal resonant frequency of dry concrete, wet concrete, and reinforced concrete is 5.95 MHz, 5.81 MHz, and 5.50 MHz, respectively. Since the power amplifier is used to adjust the resonant frequency directly in the experiment, it will lead to the loss of the transmission efficiency. However, it does not hinder the overall agreement with the simulation result.

In Figure 14, the transmission efficiency remains stable in a small scope and decreases rapidly with the gradual increase of radial offset distance. And the decreasing trend of transmission efficiency remains basically consistent with the increase of radial offset distance. According to the optimization scheme, the resonant frequency is adjusted to the optimal resonant frequency in different concrete conductivity, and the transmission efficiency is improved to a certain extent which has the most obvious effect on wireless power transfer in reinforced concrete. When the dislocation angle α varies from 0° to 45°, the transmission performance remains steady in Figure 15 which still proves the effectiveness of the proposed optimization scheme.

5. Results

The effects of radial offset and axial dislocation on the transmission performance in different concrete conductivity were analyzed. With the increase of radial offset distance, the transmission efficiency decreased dramatically. When the dislocation angle α varied from 0° to 45°, the fluctuation of the transmission efficiency was small. And the effect of concrete conductivity on the transmission efficiency was holistic. The transmission efficiency has overall decrease with the continuous increase of concrete conductivity at different radial offset and axial dislocation.

The relationship between the resonant frequency and the transmission efficiency in different concrete conductivity was analyzed; an optimization scheme was proposed. The optimal resonant frequency was gradually decreasing with the increase of conductivity. The frequency shift was also an important factor that caused the change of transmission performance. Thus, when the transmission efficiency was lower than the normal transmission standard in engineering due to the change of coil position or the difference of concrete conductivity, the transmission efficiency could be improved by properly reducing resonant frequency to close the optimal resonant frequency.

6. Discussion

This paper studied and optimized the asymmetric wireless power transfer system in concrete in the context of the concrete structural health monitoring network. Through the proposal of the eddy current equivalent resistance and corrected mutual inductance voltage, the influencing factors of transmission efficiency were simplified. The effects of radial

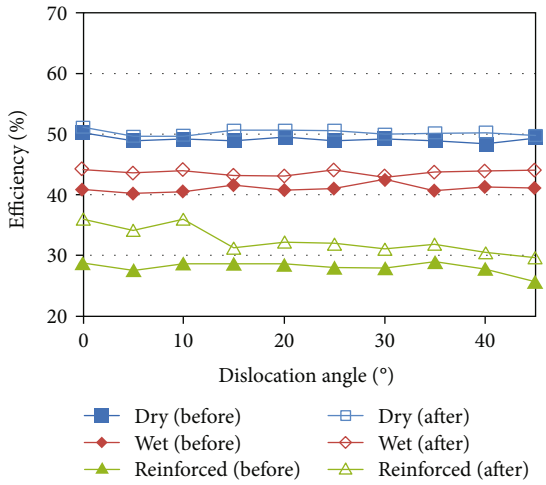

FIGURE 15: The effect of axial dislocation on the transmission efficiency in different concrete medium.

offset and axial dislocation on the transmission efficiency in different concrete conductivity were further analyzed by establishing the field-circuit coupled model. Through the relationship between the resonant frequency and the transmission efficiency in different concrete conductivity, and an optimization scheme was proposed to improve the transmission performance. Finally, the experimental setups were established, and the theoretical analysis was verified, which not only promoted the development of the concrete structural health monitoring network but also enriched the power solutions of IoT. With the continuous development of wireless power transfer technology, its deep integration with the IoT ecosystem will further reduce the production cost of products and improve the coverage of the IoT.

Although the correctness of the optimization scheme in concrete medium has been verified, it is uncertain whether the scheme is effective for the wireless power supply system of IoT under other transmission media. The relationship between the resonant frequency and the transmission efficiency in various transmission media will become the further research direction in the future.

Data Availability

The data used to support the findings of this study are available from the corresponding author upon request.

Conflicts of Interest

The authors declare that they have no conflicts of interest.

Acknowledgments

This work was funded by the National Natural Science Foundation of China, grant number 52074305 and 51874300; National Natural Science Foundation of China and Shanxi Provincial People's Government Jointly Funded Project of China for Coal Base and Low Carbon, grant number U1510115; and the Open Research Fund of Key Laboratory of Wireless Sensor Network & Communication, Shanghai Institute of Microsystem and Information Technology, Chinese Academy of Sciences, grant numbers 20190902 and 20190913.

References

[1] X. Kong, Y. Xu, Z. Jiao, D. Dong, X. Yuan, and S. Li, "Fault location technology for power system based on information about the power internet of things," *IEEE Transactions on Industrial Informatics*, vol. 16, no. 10, pp. 6682–6692, 2020.

[2] M. Choksi and M. A. Zaveri, "Multiobjective based resource allocation and scheduling for postdisaster management using IoT," *Wireless Communications and Mobile Computing*, vol. 2019, Article ID 6185806, 16 pages, 2019.

[3] Z. Safdar, S. Farid, M. Qadir, K. Asghar, J. Iqbal, and F. K. Hamdani, "A novel architecture for internet of things based E-health systems," *Journal of Medical Imaging and Health Informatics*, vol. 10, no. 10, pp. 2378–2388, 2020.

[4] A. Kurs, A. Karalis, R. Moffatt, J. D. Joannopoulos, P. Fisher, and M. Soljacic, "Wireless power transfer via strongly coupled magnetic resonances," *Science*, vol. 317, no. 5834, pp. 83–86, 2007.

[5] L. Tan, K. E. I. Elnail, M. Ju, and X. Huang, "Comparative analysis and design of the shielding techniques in WPT systems for charging EVs," *Energies*, vol. 12, no. 11, p. 2115, 2019.

[6] V. Cirimele, F. Freschi, L. Giaccone, L. Pichon, and M. Repetto, "Human exposure assessment in dynamic inductive power transfer for automotive applications," *IEEE Transactions on Magnetics*, vol. 53, no. 6, pp. 1–4, 2017.

[7] F. Lu, H. Zhang, C. Zhu et al., "A Tightly Coupled inductive power transfer system for low-voltage and high-current charging of automatic guided vehicles," *IEEE Transactions on Industrial Electronics*, vol. 66, no. 9, pp. 6867–6875, 2019.

[8] D. Kim, D. Jeong, J. Kim et al., "Design and implementation of a wireless charging-based cardiac monitoring system focused on temperature reduction and robust power transfer efficiency," *Energies*, vol. 13, no. 4, p. 1008, 2020.

[9] K. M. Z. Shams and M. Ali, "Wireless power transmission to a buried sensor in concrete," *IEEE Sensors Journal*, vol. 7, no. 12, pp. 1573–1577, 2007.

[10] J.-M. Kim, M. Han, H. J. Lim, S. Yang, and H. Sohn, "Operation of battery-less and wireless sensor using magnetic resonance based wireless power transfer through concrete," *Smart Structure and Systems*, vol. 17, no. 4, pp. 631–646, 2016.

[11] Z. Wang, O. Kypris, and A. Markham, "RePWR: wireless power transfer within reinforced concrete," in *Proceedings of the 4th International Workshop on Energy Harvesting and Energy-Neutral Sensing Systems*, pp. 1–6, California, CA, USA, 2016.

[12] H. Ishida and H. Furukawa, "Wireless power transmission through concrete using circuits resonating at utility frequency of 60 Hz," *IEEE Transactions on Power Electronics*, vol. 30, no. 3, pp. 1220–1229, 2015.

[13] S.-H. Lee, M.-Y. Kim, B.-S. Lee, and J. Lee, "Impact of rebar and concrete on power dissipation of wireless power transfer systems," *IEEE Transactions on Industrial Electronics*, vol. 67, no. 1, pp. 276–287, 2020.

[14] Y. Jang, J.-K. Han, J.-I. Baek, G. Moon, J.-M. Kim, and H. Sohn, "Novel multi-coil resonator design for wireless power transfer through reinforced concrete structure with rebar

array," in *2017 IEEE 3rd International Future Energy Electronics Conference and ECCE Asia (IFEEC 2017 - ECCE Asia)*,, pp. 2238–2243, Kaohsiung, Taiwan, 2017.

[15] X. H. Jin, J. M. Caicedo, and M. Ali, "Near-field wireless power transfer to embedded smart sensor antennas in concrete," *Applied Computational Electromagnetics Society Journal*, vol. 30, no. 3, pp. 261–269, 2015.

[16] R. H. Bhuiyan, R. Islam, J. M. Caicedo, and M. Ali, "A study of 13.5-MHz coupled-loop wireless power transfer under concrete and near metal," *IEEE Sensors Journal*, vol. 18, no. 23, pp. 9848–9856, 2018.

[17] J.-M. Kim, M. Han, and H. Sohn, "Magnetic resonance-based wireless power transmission through concrete structures," *Journal of Electromagnetic Engineering and Science*, vol. 15, no. 2, pp. 104–110, 2015.

[18] O. Jonah and S. V. Georgakopoulos, "Wireless power transfer in concrete via strongly coupled magnetic resonance," *IEEE Transactions on Antennas and Propagation*, vol. 61, no. 3, pp. 1378–1384, 2013.

[19] S. R. Khan, S. K. Pavuluri, and M. P. Y. Desmulliez, "Accurate modeling of coil inductance for near-field wireless power transfer," *IEEE Transactions on Microwave Theory and Techniques*, vol. 66, no. 9, pp. 4158–4169, 2018.

[20] B. K. Kushwaha, G. Rituraj, P. Kumar, and P. Bauer, "Mathematical model for the analysis of series-parallel compensated wireless power transfer system for different misalignments," *IET Circuits, Devices & Systems*, vol. 13, no. 7, pp. 970–978, 2019.

[21] F. Liu, Y. Yang, D. Jiang, X. Ruan, and X. Chen, "Modeling and optimization of magnetically coupled resonant wireless power transfer system with varying spatial scales," *IEEE Transactions on Power Electronics*, vol. 32, no. 4, pp. 3240–3250, 2017.

[22] P. Gao, Z. Tian, T. Pan, J. Wu, and W. Gui, "Transmission efficiency analysis and optimization of magnetically coupled resonant wireless power transfer system with misalignments," *AIP Advances*, vol. 8, no. 8, 2018.

[23] Z. Zhang and B. Zhang, "Angular-misalignment insensitive omnidirectional wireless power transfer," *IEEE Transactions on Industrial Electronics*, vol. 67, no. 4, pp. 2755–2764, 2020.

[24] D. Liu and S. V. Georgakopoulos, "Cylindrical misalignment insensitive wireless power transfer systems," *IEEE Transactions on Power Electronics*, vol. 33, no. 11, pp. 9331–9343, 2018.

[25] L. Murliky, R. W. Porto, V. J. Brusamarello, F. R. de Sousa, and A. Triviño-Cabrera, "Active tuning of wireless power transfer system for compensating coil misalignment and variable load conditions," *AEU - International Journal of Electronics and Communications*, vol. 119, article 153166, 2020.